Kinetics of Heterogeneous Electron Transfer Reactions at the Externally Polarized Water/o-Nitrophenyl Octyl Ether Interface

ARTICLE *in* THE JOURNAL OF PHYSICAL CHEMISTRY C · OCTOBER 2008

Impact Factor: 4.77 · DOI: 10.1021/jp802435m

8 AUTHORS, INCLUDING:

Shubao Xie
Peking University
14 PUBLICATIONS **532** CITATIONS
SEE PROFILE

Bo Li
Nanjing University
394 PUBLICATIONS **3,379** CITATIONS
SEE PROFILE

Meixian Li
Peking University
97 PUBLICATIONS **3,224** CITATIONS
SEE PROFILE

Yuanhua Shao
Peking University
98 PUBLICATIONS **3,234** CITATIONS
SEE PROFILE

Kinetics of Heterogeneous Electron Transfer Reactions at the Externally Polarized Water/*o*-Nitrophenyl Octyl Ether Interface

Shubao Xie, Xin Meng, Zhongwei Liang, Bo Li, Zhong Chen, Zhiwei Zhu, Meixian Li, and Yuanhua Shao*

Beijing National Laboratory for Molecular Sciences, Institute of Analytical Chemistry, College of Chemistry and Molecular Engineering, Peking University, Beijing 100871, China

Received: March 19, 2008; Revised Manuscript Received: August 26, 2008

The heterogeneous electron transfer (ET) reactions between dimethylferrocenium ($DiMFc^+$) or ferrocenium (Fc^+) produced in situ in *o*-nitrophenyl octyl ether (NPOE) and hexacyanoferrite [$Fe(CN)_6^{4-}$] in aqueous phase have been investigated by scanning electrochemical microscopy (SECM). The potential difference across the water/NPOE (W/NPOE) interface was controlled externally to maintain a certain driving force for the ET reactions. The standard kinetic rate constants (k_{12}^0) for the above bimolecular ET reactions were measured to be 0.075 and 0.050 cm s^{-1} M^{-1} when DiMFc and Fc were employed as the respective organic reactants. The transfer coefficients (α) were calculated to be 1.09 and 1.62, respectively. Those abnormal values of α were analyzed and ascribed to the Frumkin effect (or diffuse layer effect) at both sides of the interfaces. Some of the previous reports are summarized and also analyzed based on the Frumkin effect. The possible effect of ion transfer on the ET process is discussed in detail.

Introduction

There have been a number of investigations of heterogeneous electron transfer (ET) processes at liquid/liquid (L/L) interfaces (or interfaces between two immiscible electrolyte solutions, ITIES) in the past more than two decades because such studies can offer the possibility of elucidating the mechanisms of interfacial processes and the fundamentals of interfacial structures.[1] Some electrochemical techniques, including cyclic voltammetry,[2] ac impedance,[3] thin layer cell voltammetry (TLCV),[4] microelectrochemical measurements at expanding droplets (MEMED),[5] spectroscopic and photoelectrochemical techniques,[6] and scanning electrochemical microscopy (SECM),[7] have been employed to study the ET processes. Among these techniques, SECM has played a key role in the investigation of the potential dependence of the ET kinetics, since the pioneering work by Bard et al.,[8] for the reason that SECM measurements are essentially free of complications caused by *iR* drop and the charging current due to the application of ultramicroelectrodes (UMEs) as the SECM tip. One of the focuses in these SECM studies is the dependence of the ET kinetic rate constant on the potential difference across the interface. It has been demonstrated that the kinetic behavior of most of the ET reactions taking place at a L/L interface can be described in terms of the Butler−Volmer equation at lower driving forces, and the Marcus theory[9] of ET, at higher driving forces. The potential-independent ET rate constants were also reported by Liu and Mirkin[10] using SECM and by Shi and Anson using TLCV.[4a] To clarify the potential dependence of the ET reaction, Unwin et al. carried out experimental studies for many systems, and their efforts in SECM methodology extended the range of processes and conditions that might be studied by SECM.[11,12] They also explained that the results obtained by Shi and Anson[4a] were due to the diffusion limitation.[4b]

In the previous SECM kinetic investigations, the nonpolarized liquid/liquid interfaces have often been employed, and the interfacial potential drop was controlled by variation of the concentration of a common ion in one of the two phases. In this case, SECM measurements are free of complications caused by an *iR* drop, since there is no externally applied potential across the interface. However, the range of the controllable potential is limited, and the change in concentration of common ions in solutions sometimes makes the data analysis difficult. Shao's group has combined the conventional electrochemistry at L/L interfaces with SECM, introduced the SECM experiment at externally polarized liquid/liquid interface, and observed the Marcus inverted region with a single redox pair, mainly because of the wide range of available potential difference.[13] Furthermore, Quinn et al. designed a new cell configuration and facilitated the SECM measurements at the polarized L/L interfaces.[14]

Although after many years of investigations concerning this aspect, the dependence of the heterogeneous ET reactions on the potential difference is still confusing due to the lack of exact knowledge of the interfacial structure, especially the potential distribution within the interfacial region, which determines whether the observed relationship of potential dependence should be ascribed to kinetic or to thermodynamic aspects, the former leading to the Butler−Volmer-type or the Marcus-type interpretation and the latter to applications of diffuse layer effect.[15] At present, one of the most popular models of a L/L interface was presented by Girault and Schiffrin,[16] in which the interface is supposed to be composed of two diffuse layers and an inner layer (also called mixed solvent layer), and the potential drop develops mainly at the two diffuse layers. A piece of excellent work has been conducted by Girault's group,[6a] in which the potential dependence of an ET reaction was demonstrated to be involved in both of the two aspects, that is, the diffuse layer effect and Butler−Volmer kinetics, and the ratio of the potential drop in the inner layer was estimated to be nearly

* To whom the correspondence should be addressed. E-mail: yhshao@pku.edu.cn.

10.1021/jp802435m CCC: $40.75
Published on Web 10/25/2008

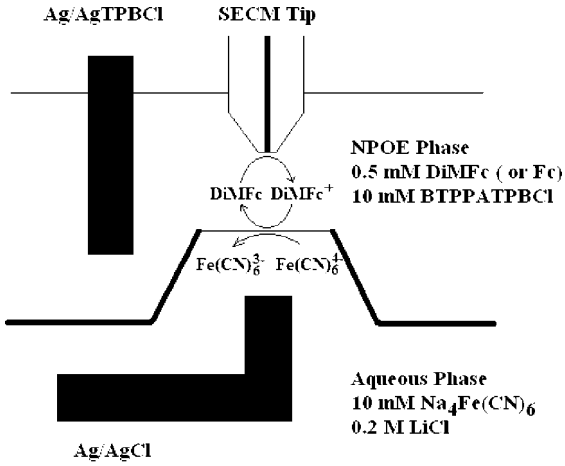

Figure 1. Measurements of the kinetics of the interfacial reaction between DiMFc $^+$ (or Fc^+) in NPOE and $Fe(CN)_6^{4-}$ in water with the SECM operating in feedback mode.

30% within the experimental potential range by means of spectroelectrochemical approaches combined with electrostatic calculation.

A better understanding can be achieved by comparing the kinetics of ET measured at different interfaces. The most frequently used organic phase is 1,2-dichloroethane (DCE), and some other organic solvents, including nitrobenzene (NB),[11a,d,17] chlorobenzene (CB),[11c,14] benzonitrile,[18] and benzene,[17] have been employed, as well. More recently, Mirkin[19] et al. used an ionic liquid, 1-octyl-3-methylimidazolium bis(trifluoromethylsulfonyl)imide, and its mixture with DCE as the organic phases and observed an abnormally larger bimolecular rate constant at the water/ionic liquid interface than that at the W/DCE interface, which they attributed to the particular phase boundary. On the other hand, the W/NPOE interface has attracted some attention from several groups in the realm of both ET[20] and ion transfer[21] because of NPOE's low volatility and much lower miscibility with water and less toxicity than that of conventional solvents; for example, DCE. Quinn et al.[20a] studied for the first time the ET reactions at the macro- and micro-W/NPOE interfaces using cyclic voltammetry and found that ET involving DiMFc was reversible, whereas that involving Fc or TCNQ was quasi-reversible, and that the micro ITIES were not amenable to kinetic determination. Nakatani et al.[20c] investigated the ET between hexacyanoferrate [$Fe(CN)_6^{3-}$] and a ferrocene derivative at nonpolarized micro-water-droplet/NPOE interface by cyclic voltammetry and obtained a negative dependence of the ET rate constant on the Gibbs energy, which was ascribed to the Marcus inverted region. The possible influence of transfer of ion due to the ET on the ET process at this interface was mentioned. However, there are no SECM studies and no reliable kinetic data obtained for the ET reaction at the polarized W/NPOE interface, as far as we know.

In this work, the heterogeneous ET kinetic rate constants for the reaction between $DiMFc^+$ (or Fc^+) and $Fe(CN)_6^{4-}$ at the externally polarized W/NPOE interface have been measured by SECM for the first time. A schematic diagram of the SECM experiment is given in Figure 1. The transfer coefficients (α) were calculated to be 1.09 and 1.62, respectively. These abnormal values of α have been discussed and ascribed to the Frumkin effect (or diffuse layer effect) at both sides of the interface. We also analyzed some data from the previous reports on the basis of the Frumkin effect and the interfacial model proposed by Girault and Schiffrin and compared them with our experimental results. The transfers of $DiMFc^+$ and Fc^+ have been observed experimentally for the first time by micropipet voltammetry, and their possible effect on the ET process was discussed in detail, as well.

Experimental Section

Chemicals. Sodium hexacyanoferrite [$Na_4Fe(CN)_6 \cdot 10H_2O$, 99%, Sigma-Aldrich], potassium hexacyanoferrite ($K_4Fe(CN)_6 \cdot 3H_2O$, 99.5%,) and potassium hexacyanoferrate ($K_3Fe(CN)_6$, 99.5%) (Beijing Chemical Co., Beijing, China), ferrocene (Fc, 98%, Acros), and dimethylferrocene (DiMFc, 97%, Aldrich) were used as redox couples. The supporting electrolyte in the organic phase, bis(triphenylphosphoranylidene)ammonium tetrakis(4-chlorophenyl)borate (BTPPATPBCl), was prepared via the metathesis of bis(triphenylphosphoranylidene) ammonium chloride (BTPPACl, Selectophore, Fluka) and potassium tetrakis(4-chlorophenyl)borate (KTPBCl, Selectophore, Fluka) as described previously.[22] Tetrabutylammonium tetrakis(4-chlorophenyl)borate (TBATPBCl) was prepared by the same method using KTPBCl and tetrabutyl ammonium chloride (TBACl, 97%, Fluka). 2-Nitrophenyl octyl ether (NPOE, 99%, Fluka) was used as the organic solvent. Aqueous solutions were prepared using deionized water (Milli-Q, Millipore Corp. Billirica, MA). The supporting electrolyte in the aqueous phase was lithium chloride ($LiCl \cdot xH_2O$, 99%, Beijing Chemical Co., Beijing, China). All the reagents were analytical grade or better and were used as received.

Electrodes and Electrochemical Cells. The following electrochemical cell was used to obtain the potential window in cyclic voltammetric experiments and to maintain a certain interfacial potential in SECM experiments, where || refers to the polarizable interface under study:

$$\begin{aligned} &\text{Ag|AgTPBCl||0.5 mM DiMFc (or Fc),} \\ &\quad x \text{ mM TBATPBCl,10 mM BTPPATPBCl(NPOE)||} \\ &\quad 10\text{mM } Na_4Fe(CN)_6\text{, 0.2 M LiCl(water)|AgCl|Ag} \end{aligned} \qquad \text{Cell 1}$$

The platinum ultramicroelectrode (Pt UME) employed in the cyclic voltammetric and SECM experiments was prepared by heating and sealing a Pt wire (10 μm in diameter, Good Fellow Co.) in a glass capillary under vacuum, followed by polishing and sharpening as described previously.[23] An Olympus BX-51 optical microscope was used to examine the prepared tip. The Rg value of the tip (Rg = b/a, where a is the radius of the Pt wire and b is the radius of the surrounding glass) in these experiments is about 3. A specially designed setup introduced by Liljeroth et al.[14] was used to carry out kinetic measurements in which a L/L interface supported at the tip of a glass capillary of 400 μm i.d. was used as the SECM substrate because it is both large enough compared to the diameter of the SECM tip and small enough to get a negligible iR drop in the two-electrode system. Two silver wires (0.4 mm in diameter) coated with AgCl and AgTPBCl, respectively, acted as references, one in the organic phase and the other in the aqueous phase. The organic solutions were always used as the upper phase, and the aqueous solutions, as the lower phase.

A model P-2000 laser puller (Sutter Instruments) was used to fabricate micropipets with an orifice radius in the range of 2−10 μm from borosilicate glass capillaries (o.d./i.d., 1.0/0.58 mm); this was done by controlling the pulling parameters. The aqueous solution was filled from the back of the micropipet using a 10 μL syringe. The micropipet was inspected with an optical microscope (BX-51, Olympus) prior to each measurement; this inspection was also used to measure the orifice radius

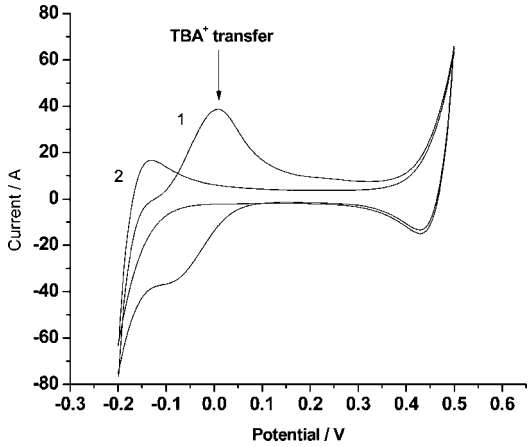

Figure 2. The cyclic voltammogram obtained at the polarized W/NPOE interface supported at a glass capillary (i.d., 400 μm) using cell 1 ($x = 0$ for curve 1; $x = 0.5$ for curve 2, where TBA^+ is used as an internal reference ion). The scan rate is 20 mV/s.

and to ensure there were no bubbles trapped inside. A Pt electrode (CH Instruments, Inc.) with a diameter of 2 mm was used as a substrate electrode to produce $DiMFc^+$ and Fc^+ in the SECM generation/collection (G/C) experiments.[24]

SECM Apparatus and Procedures. The electrochemical measurements were performed with a CHI 900 SECM setup (CH Instruments, Inc.). In the SECM kinetic measurements, all electrodes except the Ag/AgCl electrode were positioned within the top phase (NPOE), the tip was biased at a potential where the ET reaction is diffusion-controlled, and the substrate electrode (the interface) was biased within the potential window of the system (see more details in the Discussion section). The experimental approach curves were obtained by moving the tip toward the interface and recording the tip current (i_T) as a function of the distance between the tip and the interface (d). The closest distance between the tip and the ITIES was determined by running a pure negative approach curve and analyzing the data with negative feedback theory. All experiments were conducted at room temperature (22 $\pm$ 2 °C).

In the SECM G/C experiments, a micropipet was used as the tip/collection electrode and positioned at a distance of about 10 μm from the big Pt substrate electrode using the feedback mode of the transfer of TBA^+ from outside the micropipet to inside, which was also used as the inner reference ion (cell 4). The potential of the substrate electrode was kept at a value where DiMFc or Fc can be oxidized.

Results and Discussion

The ET Driving Force and Possible Influence of $DiMFc^+$ and Fc^+. A cyclic voltammogram obtained at the externally polarized interface supported at the tip of the 400-μm-diameter glass capillary with cell 1 is shown in Figure 2 (DiMFc as the organic redox species, and Fc was much alike). The available potential window in this system is about 500 mV wide (from -100 to 400 mV). The current in the middle of the potential window is less than 10 nA. When conducting SECM experiments, the potential (SECM substrate potential) is kept at a certain value within this range, and the substrate current and the tip current are recorded in the nanoampere level when the tip approaches the interface. The *iR* drop across the interface was measured to be about 7×10^5 Ω using CHI 660A (CH Instruments, Inc.) before SECM experiments. Thus, the *iR* drop is within 1 mV and can be neglected. After finishing the cyclic voltammetray (curve 1 in Figure 2), 0.5 mM TBATPBCl was added to the NPOE phase, and the TBA^+ acts as an internal reference ion (curve 2 in Figure 2), which can be used to compare with the results obtained in Figure 3.

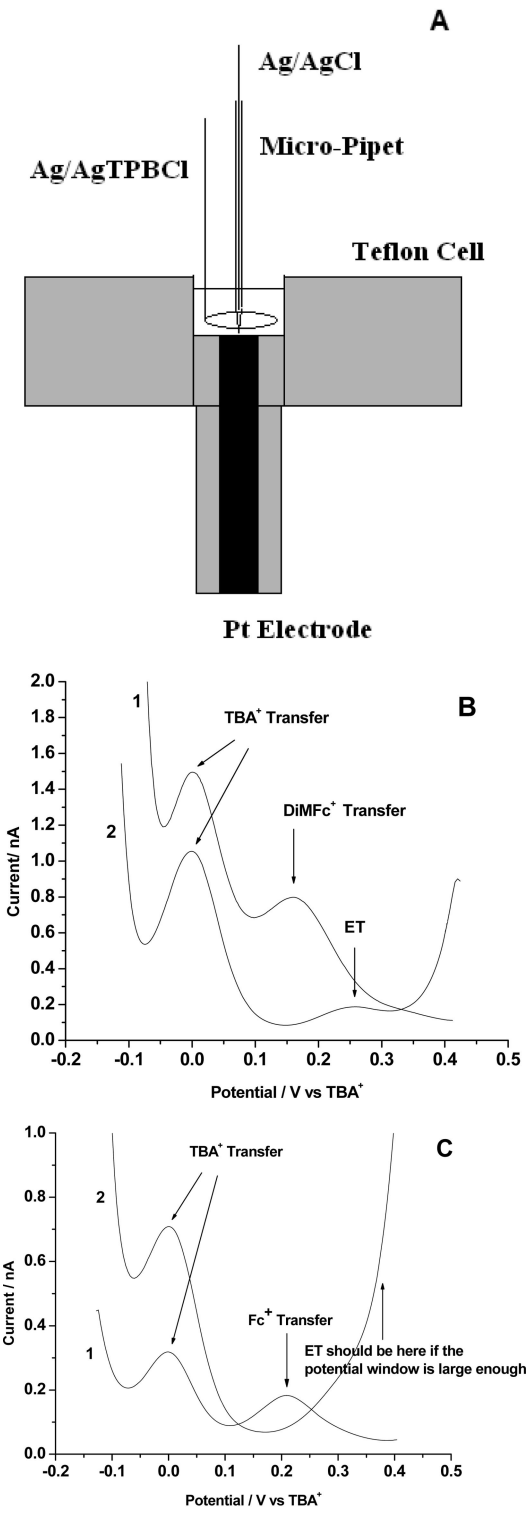

Figure 3. (A) The schematic diagram for SECM G/C experiments. (B) Differential pulse voltammograms of $DiMFc^+$ transfer (curve 1, using cell 4, in SECM G/C mode) and of electron transfer between $Fe(CN)_6^{3-}$ and DiMFc (curve 2, using cell 5) at the NPOE/water interface supported at several-micron diameter pipets. Modulation amplitude, 0.05 V; step potential, 0.004 V; scan rate, 0.02 V/s. (C) The same as B, except that Fc is used instead of DiMFc.

In the Supporting Information of ref 13b, the authors provided a method to evaluate the relationship between the driving force

(DF) and applied potential. For our system, the DF can be expressed by

$$\mathrm{DF} = -E_o^w + E_{1/2}^0 - E_{1/2}^w \quad (1)$$

where E_0^w is the externally applied potential and $E_{1/2}^0$ and $E_{1/2}^w$ are the half-wave potentials obtained by cyclic voltammograms using cells 2 and 3, respectively:

Ag|AgTPBCl|0.5 mM DiMFc (or Fc), 10 mM BTPPATPBCl(NPOE)|$Pt_{microtip}$

Cell 2

Ag|AgCl|10 mM$Na_4Fe(CN)_6$, 0.2 M LiCl (water)|$Pt_{microtip}$

Cell 3

where the $Pt_{microtip}$ is the SECM tip. The values of $E_{1/2}^0$(DiMFc), $E_{1/2}^0$(Fc), and $E_{1/2}^w$ were measured to be 0.418, 0.538, and 0.178 V, respectively. On the basis of eq 1, the driving forces of the two reactions were

$$\mathrm{DF\ (DiMFc)} = 0.240\ \mathrm{V} - E_0^w \quad (2)$$

$$\mathrm{DF\ (Fc)} = 0.360\ \mathrm{V} - E_0^w \quad (3)$$

Whether the ion produced by the ET process can influence the ET is still a matter of controversy. There have been reports that both systems DiMFc(O)/$Fe(CN)_6^{3/4-}$(W) and Fc(O)/$Fe(CN)_6^{3/4-}$(W) are ideal ones, and there was no influence from IT to ET,[6a] but there were also reports they could influence each other.[25] In the previous studies, the stability of the produced ions in organic phase[2a,25a,c] and the effect of supporting electrolytes have been discussed.[2a,26] Actually, both systems at the water/1,2-dichloroethane (W/DCE) and water/nitrobenzene (W/NB) are rather complicated. Although there were several reports regarding the ET at the W/NPOE interface, there was no direct observation of IT (the transfer of $DiMFc^+$ and Fc^+) reported.

To study such a problem, we have designed a special cell (see Figure 3A) by which the DiMFc (or Fc) can be oxidized to $DiMFc^+$ (or Fc^+) by controlling the potential on the Pt electrode, whereas a micropipet filled with only aqueous supporting electrolyte can be used to collect the IT:

$$\underbrace{\mathrm{Ag\ |\ AgCl\ |\ 0.2\ M\ LiCl\ |}}_{\text{(inside micropipet, aqueous phase)}}$$
$$\underbrace{\mathrm{|\ 2mM\ DiMFc, 1mM\ TBATPBCl, 10mM\ BTPPATPBCl\ |\ AgTPBCl\ |\ Ag}}_{\text{(outside micropipet, NPOE phase)}}$$

Cell 4

Figure 3B1 shows the differential pulse voltammogram (DPV) of $DiMFc^+$ transfer at the W/NPOE interface and its potential related to the TBA^+ (as an internal reference ion). Using the following cell 5, the ET between DiMFc and $Fe(CN)_6^{3/4-}$ can also be studied, and its DPV is shown in Figure 3B2. The potential of ET is about 96 mV higher than that of IT, which is similar to that system of W/DCE (~94 mV).[27] This difference means that the ET reaction may be disturbance-free from IT at a higher potential.

$$\underbrace{\mathrm{Ag\ |\ AgCl\ |\ 20\ mM\ K_3Fe(CN)_6, 2\ mM\ K_4Fe(CN)_6, 0.2\ M\ LiCl\ ||}}_{\text{(inside micropipet, aqueous phase)}}$$
$$\underbrace{\mathrm{2\ mM\ DiMFc, 1\ mM\ TBATPBCl, 10\ mM\ BTPPATPBCl\ |\ AgTPBCl\ |\ Ag}}_{\text{(outside micropipet, NPOE phase)}}$$

Cell 5

TABLE 1: The Potentials of ET and IT of DiMFc/$Fe(CN)_6^{3/4-}$ and Fc/$Fe(CN)_6^{3/4-}$ Systems vs TBA^+ Transfer at the W/NPOE Interface

	IT	ET	ET−IT	ET−IT at W/DCE interface in ref 27
DiMFc	160 mV	256 mV	96 mV	94 mV
Fc	212 mV	376 mV	164 mV	150 mV

Similarly, the system Fc/$Fe(CN)_6^{3/4-}$ was also studied by the same methodology. Figure 3C1 shows the DPV of transfer of Fc^+ at the W/NPOE interface. Although we did not observe the ET process for this system, on the basis of eqs 2 and 3, the potential of ET of the Fc system shall be 120 mV more positive than that of DiMFc, and the potential difference between IT and ET shall be about 164 mV, close to the results at the W/DCE interface (~150 mV).[27] These results are listed in Table 1. The potential windows in Figure 3 are slightly different from that in Figure 2, and it is due to the electrochemical cells' being different. These results can be compared on the basis of the same internal reference ion (TBA^+).

SECM Measurements at the Externally Polarized L/L Interface. The SECM can be used to determine precisely the magnitude of the heterogeneous ET rate constant of a reaction taking place at an interface when the SECM tip is approaching it and to obtain a feedback current caused by the reaction between the SECM tip and the interface, which is called the SECM feedback mode.[23] The kinetic rate constant can be extracted from the fitting of an experimental $i_T - d$ curve (or called an approach curve, in which i_T is the tip current and d the distance between the tip and the substrate) to the theoretical one. It has been found that the theoretical $i_T - d$ response can be accurately described by the following equations,[8b]

$$I_T^k = I_S^k(1 - I_T^{ins}/I_T^c) + I_T^{ins} \quad (4)$$

where

$$I_S^k = 0.78377/L(1 + 1/\Lambda) + (0.68 + 0.3315\exp\times (-1.0672/L))/(1 + F(L,\Lambda)) \quad (5)$$

The analytical approximations of I_T^k and I_T^{ins} vary with the Rg value of the tip, and we selected the expressions for $Rg = 5.1$ (the closest to the real Rg of our tip in literature) given by Amphlett and Denuault.[28]

$$I_T^c = 0.72035 + 0.75128/L + 0.26651\exp(-1.62091/L) \quad (6)$$

$$I_T^{ins} = 1/[0.48678 + 1.17706/L + 0.51241\exp\times (-2.07873/L)] \quad (7)$$

In the above four equations, the tip currents have been normalized by the steady-state current obtained when the tip is far from the substrate ($I_T = i_T/i_{T,\infty}$), and the distance is made dimensionless by dividing by the tip electrode radius ($L = d/a$). I_T^k, I_T^c, and I_T^{ins} denote the normalized tip currents for finite substrate kinetics, diffusion-controlled regeneration of a redox mediator, and insulating substrate, respectively. I_S^k is the kinetically controlled normalized substrate current. Λ equals $k_f a/D$, where k_f is the heterogeneous rate constant in centimeters per second, and D is the diffusion coefficient of the regenerated species. $F(L,\Lambda)$ is given by

$$F(L,\Lambda) = (11 + 7.3\Lambda)/[\Lambda(110 - 40L)] \quad (8)$$

For a SECM feedback experiment at a L/L interface the constant-composition approximation should be kept valid to

ensure the validity of eqs 4–8, that is, as suggested by Barker et al.,[12b] the concentration of the redox species in the lower phase should be not less than 15−20 times that in the upper phase, provided that the diffusion coefficients of the redox reactants in the two phases are similar and the discussion can be simplified.

In this work, we implemented the following ET reactions at the W/NPOE interface:

$$\mathrm{DiMFc^+\ (or\ Fc^+,\ in\ NPOE)} + \mathrm{Fe(CN)_6^{4-}\ (in\ water)} \rightarrow \mathrm{DiMFc\ (or\ Fc,\ in\ NPOE)} + \mathrm{Fe(CN)_6^{3-}\ (in\ water)} \quad (9)$$

$DiMFc^+$ (or Fc^+) was produced at the SECM tip under diffusion-controlled conditions, diffused to the substrate (i.e., the W/NPOE interface), and reacted with $Fe(CN)_6^{4-}$ at the interface. The relationship between the apparent heterogeneous rate constant for reaction 9, k_f, which can be determined by the SECM i_T-d curve, and the bimolecular ET rate constant, k_{12}, is as follows,

$$k_f = k_{12} c_{Fe(CN)_6^{4-}} \quad (10)$$

where $c_{Fe(CN)_6^{4-}}$ is the concentration of $Fe(CN)_6^{4-}$ in the aqueous phase. The diffusion coefficients of DiMFc in NPOE, Fc in NPOE, and $Fe(CN)_6^{4-}$ in water were measured to be 7.9×10^{-7}, 9.0×10^{-7}, and 6.0×10^{-6} cm^2/s, respectively, by steady-state voltammetry using cells 2 and 3. The diffusion coefficients of $DiMFc^+$ and Fc^+ used in SECM simulation were supposed to be the same as those of DiMFc and Fc. In fact, though the unequal diffusion coefficients of the redox couple have been reported,[29] the difference between them in conventional solvents is not very remarkable (as an example, the ratio of Fc^+/Fc is 80% in acetonitrile[29a]). The more important problem for SECM is that, as pointed out by Unwin et al.,[29a] this difference will possibly lengthen the time to reach steady state and, thus, affect the approach curves when the approach rate is high. Fortunately, this was not the case, and no obvious difference was found in the approach curves when the approach rates ranged from 0.5 to 3 μm/s in our experiments. The concentration of $Fe(CN)_6^{4-}$ was 20 times that of DiMFc (or Fc) so as to meet with the constant-composition condition, and as an additional guarantee, the diffusion coefficient of the former was more than that of the latter.[12a,b] The potential difference across the interface was controlled by maintaining the potential of the substrate electrode at a certain value. These values were selected to be free of the influence of transfers of $DiMFc^+$ and Fc^+ (see Figure 3 and the above discussion). The approach curves are shown in Figures 4 and 6.

Potential Dependence of the ET Kinetics. Two systems have been tested on the potential dependence; that is, DiMFc (O)/$Fe(CN)_6^{4-}$ (W) and Fc (O)/$Fe(CN)_6^{4-}$ (W). In the case of DiMFc as the organic redox species, the rather wide potential window of the W/NPOE interface allows us to determine the ET rate constants at a driving force from 340 to −160 mV. However, when the DF was too large or too small, we could not obtain a reliable result using this method (constant-composition approximation). More importantly, carefully selected DF ranges can possibly avoid the effect of IT on the ET processes (see the above micropipet votammetric experimental results). The DF range in Figure 4 was ~40 to −110 mV; that is, the interfacial potential was ~216−366 mV vs TBA^+, which is much higher than the potential of the transfer of $DiMFc^+$ (160 mV vs TBA^+). The Tafel plot in the lower DF range is given in Figure 5, where

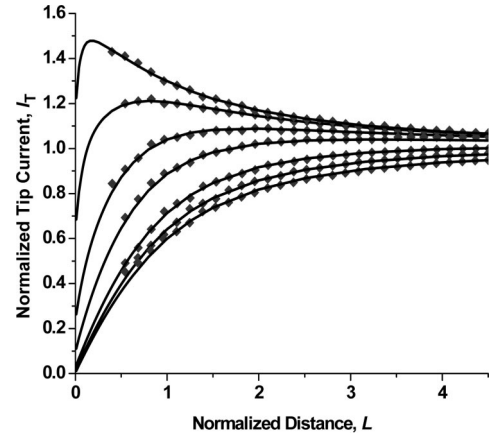

Figure 4. The approach curves at different driving forces obtained with a 10-μm-diameter Pt UME.The dotted lines are experimental approach curves, and the solid lines are the theoretical curves best fit to the experimental ones. Upper phase: 0.5 mM DiMFc/10 mM BTPPATPBCl/NPOE. Lower phase: 10 mM $Na_4Fe(CN)_6$/0.2 M LiCl/H_2O. From top to bottom, the solid experimental curves are shown for DF = 40, 15, −10, −35, −60, −85, and −110 mV. The dotted theoretical curves (top to bottom) are shown for k_{12} = 0.22, 0.12, 0.045, 0.018, 0.005, 0.002, and 0.0006 cm s^{-1} M^{-1}. The approach rate is 1 μm/s.

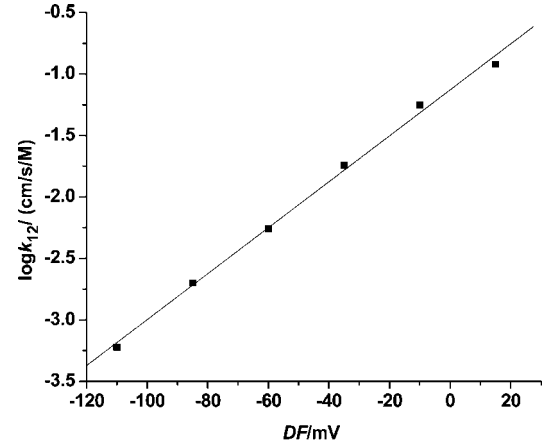

Figure 5. Driving force dependence of the ET rate constant between $DiMFc^+$ in NPOE and $Fe(CN)_6^{4-}$ in water. The NPOE phase contained 0.5 mM DiMFc and 10 mM BTPPATPBCl. The aqueous phase contained 10 mM$Na_4Fe(CN)_6$ and 0.2 M LiCl.

the logarithms of the bimolecular rate constants for reaction 9 are plotted as a function of the ET driving forces. It is clear that a Butler−Volmer relationship was followed, and linear fit to the experimental data gave a standard bimolecular rate constant, k_{12}^0; that is, the rate constant when DF is zero, 0.075 cm s^{-1} M^{-1}, and a slope (in mV/dec for convenience; i.e., $2.303RT/\alpha F$, where F is the Faraday constant, R is the universal gas constant, and T is the temperature)[30a] of 53.5 mV/dec, which means a transfer coefficient of 1.09.

Similar results were obtained when Fc was used as the organic reactant. Because the half-wave potential of Fc was higher than that of DiMFc, the SECM experiment was carried out at much higher substrate potentials. The DF range in Figure 6 was ~40 mV to −40 mV; that is, the interfacial potential was ~336−416 mV vs TBA^+, which is much higher than the potential of the transfer of Fc^+ (212 mV vs TBA^+). The Tafel plot is shown in Figure 7. The standard bimolecular rate constant was 0.050 cm s^{-1} M^{-1}, and the transfer coefficient was 1.62. These kinetic parameters for both Fc and DiMFc are summarized in Table 2. The k_{12}^0 of Fc was

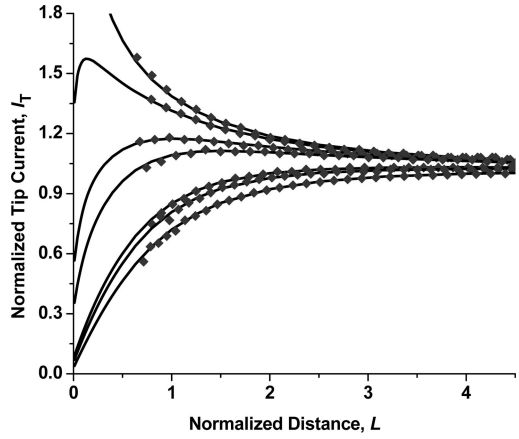

Figure 6. The approach curves at different driving forces obtained with a 10-μm-diameter Pt UME.The dotted lines are experimental approach curves, and the solid lines are the theoretical curves best fit to the experimental ones. Upper phase: 0.5 mM Fc/10 mM BTPPATPBCl/NPOE. Lower phase: 10 mM $Na_4Fe(CN)_6$/0.2 M LiCl/H2O. From top to bottom, the solid experimental curves are shown for DF = 40, 20, 10, 0, −10, −20, −30, and −40 mV. The dotted theoretical curves (top to bottom) are shown for k_{12} = 0.48, 0.27, 0.11, 0.068, 0.016, 0.012, 0.006, and 0.005 cm s^{-1} M^{-1}. The approach rate is 1 μm/s.

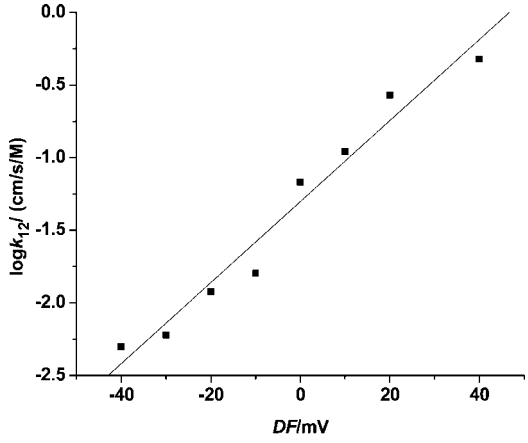

Figure 7. Driving force dependence of the ET rate constant between Fc^+ in NPOE and $Fe(CN)_6^{4-}$ in water. The NPOE phase contained 0.5 mM Fc and 10 mM BTPPATPBCl. The aqueous phase contained 10 mM $Na_4Fe(CN)_6$ and 0.2 M LiCl.

TABLE 2: Kinetic Parameters for the Heterogeneous ET Reaction between $DiMFc^+$ (or Fc^+) in NPOE and $Fe(CN)_6^{4-}$ in Water Measured by SECM

	$DiMFc^+/Fe(CN)_6^{4-}$	$Fc^+/Fe(CN)_6^{4-}$
D/(cm^2 s^{-1})	7.9×10^{-7}	9.0×10^{-7}
k_{12}^0/(cm s^{-1} M^{-1})	0.075	0.050
slope/(mV/dec)	53.3	35.8
α	1.09	1.62
$\Delta\phi_w/\Delta\phi$	0.03	0.20

slightly less than that of DiMFc, as predicted by the Marcus theory of ET, which indicates that the larger size of the reactant leads to less reorganization energy and, thus, the larger rate constants for an ET reaction.[30b]

These experimental results show abnormally large values of transfer coefficient, of which the typical value shall be about 0.5 for the Butler−Volmer model and for the Marcus model in the lower DF range.[30b] Considerable deviations from 0.5 were reported from time to time by several groups, and we have summarized some of them in Table 3. We can see that the lowest α is −1.1, and the largest is 0.94. The authors often attributed the negative α values to the Marcus inverted region[11c] or ion-pair formation.[11a] Near-zero α values were also reported and ascribed to the adsorption of the reactant at the interface[10b] or to be not a real cross-phase reaction.[4a] A very large α value is rarely reported, and we have an example in Table 3, where α is 0.94. A common feature in the systems with small α values is that the *oxidant* is a highly charged anion; in contrast, in the case of large α values (including our systems in the present work), the *reductant* is a highly charged anion. This suggests that the Frumkin effect (or diffuse layer effect) may play a key role in the potential dependence of ET kinetics, as pointed out by Mirkin et al.[10a]

The Frumkin effect was first introduced to explain some results in conventional electrochemistry with metals as the working electrodes.[30c] When the charge of a redox species ($|z|$) is not zero, the concentration of the reactant at the interface will be different from that outside the diffuse layer, C^b, but $C^b \exp(zf\Delta\phi_{diffuse})$ where $f = F/RT$, $\Delta\phi_{diffuse}$ is the potential drop in diffuse layer, R is the universal gas constant, and T is the temperature. The potential difference driving the electrode reaction is not the overall potential drop, $\Delta\phi$, but instead, $\Delta\phi - \Delta\phi_{diffuse}$. Thus, the kinetic equation should be[30c]

$$i = i_0 \exp[-\alpha_{ET}(\Delta\phi - \Delta\phi_{diffuse})f] \exp(z\Delta\phi_{diffuse}f) \quad (11)$$

or

$$i = i_0 \exp\{[-\alpha_{ET}(\Delta\phi - \Delta\phi_{diffuse})/\Delta\phi + z\Delta\phi_{diffuse}/\Delta\phi]f\Delta\phi\} \quad (12)$$

where α_{ET} is the real transfer coefficient of the ET reaction. When we use the same method for heterogeneous ET at a L/L interface, we can easily obtain the following expression,

$$i = i_0 \exp[(-\alpha_{ET}\Delta\phi_{12}/\Delta\phi + z_w\Delta\phi_w/\Delta\phi + z_o\Delta\phi_o/\Delta\phi)f\Delta\phi] \quad (13)$$

where the subscripts o and w denote the organic phase and the aqueous phase, respectively; and $\Delta\phi_{12}$, $\Delta\phi_w$, and $\Delta\phi_o$ denote the potential drops in the inner layer, the diffuse layer on the water side, and the diffuse layer on the organic side, respectively. The signs of z_w and z_o should be chosen according to the problem at hand. For a cation, the sign should be positive when acting as the oxidant and negative as the reductant. For an anion, it is just the other way around. We can extract the factor in the exponential term from eq 13 as the apparent transfer coefficient:

$$\alpha = -\alpha_{ET}\Delta\phi_{12}/\Delta\phi + z_w\Delta\phi_w/\Delta\phi + z_o\Delta\phi_o/\Delta\phi \quad (14)$$

If $\Delta\phi_{12} \approx 0$ and $\Delta\phi \approx \Delta\phi_w + \Delta\phi_o$, as predicted by the Girault−Schiffrin model,[16] we can obtain

$$\alpha \approx z_w\Delta\phi_w/\Delta\phi + z_o\Delta\phi_o/\Delta\phi \quad (15)$$

and

$$\Delta\phi_w/\Delta\phi \approx (\alpha - z_o)/(z_w - z_o) \quad (16)$$

The $\Delta\phi_w/\Delta\phi$ values listed in Table 3 are calculated by using eq 16. They have essentially a similar meaning as α_{ET}. The dielectric constant of an organic solvent is often much less than that of water, and therefore, the potential drop in aqueous phase should be less than that in the organic phase of a biphasic liquid system.[31] The calculated values of $\Delta\phi_w/\Delta\phi$ in Table 3 are from 0.017 to 0.37, which is consistent with this estimate. The $\Delta\phi_w/\Delta\phi$ values of the W/NPOE interface

TABLE 3: Some Abnormal α Values Reported by Previous Studies

α	$\Delta\phi_w/\Delta\phi$[a]	reaction	author	ref
−0.22	0.305	$C_{60}^- + Fe(CN)_6^{3-}$	Jie Zhang et al., 2001	11c (Figure 6)
0.05	0.017	$Ru(CN)_6^{3-}$ + ZnPor	Biao Liu et al., 2002	10b (Figure 6)
0.26	0.185	$TCNQ^- + Fe(CN)_6^{3-}$	Zhifeng Ding et al., 2001	8e (Figure 5)
0.94	0.24	$Fe(CN)_6^{4-}$ + TCNQ	Jie Zhang et al., 2000	11b (Figure 10)[b]
−0.44	0.147	$Fe(CN)_6^{3-}$ + DMFc	Jie Zhang et al., 2000	11a (Figure 8)[b]
−0.36	0.12	$Ru(CN)_6^{3-}$ + DMFc	Jie Zhang et al., 2000	11a (Figure 9)[b]
−1.1	0.37	$Fe(CN)_6^{3-}$ + DMFc	Jie Zhang et al., 2000	11a (Figure 11)[b]

[a] $\Delta\phi_w/\Delta\phi = (\alpha - z_o)/(z_w - z_o)$, with the assumption that the potential drop across the inner layer can be neglected. See the text. [b] The α values in ref 11a and ref 11b were recalculated using the corrected equation in the following paper: Zhang, J., Unwin, P. R. *J. Phys. Chem. B* **2001**, *105,* 11052.

TABLE 4: The Correlation between $\Delta\phi_w/\Delta\phi$ and the Ionic Strength[a]

$[NaCl]_w/[THAClO_4]_o$	0.4	1	2	20	200
$\Delta\phi_w/\Delta\phi$	0.17, 0.19	0.12, 0.16, 0.15, 0.17, 0.11	0.10	0.1, 0.02	0.08
$[Li_2SO_4]_w/[THAClO_4]_o$	1	5	15	50	
$\Delta\phi_w/\Delta\phi$	0.25, 0.2	0.17	0.07	0.14	

[a] The data are collected from refs 8, 10−14 and 17 and calculated to give the $\Delta\phi_w/\Delta\phi$ values by eq 16. The organic phases were all DCE.

TABLE 5: The Correlation between $\Delta\phi_w/\Delta\phi$ and the Dielectric Constant of the Solvent[a]

organic phase	DCE	NB
$\varepsilon/\varepsilon_0$	7.79	34.8
$\Delta\phi_w/\Delta\phi$	0.11−0.17	0.37

[a] The data are collected from refs 8, 10−14 and 17. The organic phase and the aqueous phase contained supporting electrolyte of an equivalent concentration. $\varepsilon/\varepsilon_0$ is the dielectric constant of the solvent.

in this work are 0.03 and 0.20, falling in this range. For the reverse reaction, the transfer coefficient, β, can be calculated from eq 15 directly:

$$\beta \approx (1 - z_w)\Delta\phi_w/\Delta\phi + (1 - z_o)\Delta\phi_o/\Delta\phi$$
$$= (\Delta\phi_w/\Delta\phi + \Delta\phi_o/\Delta\phi) - (z_w\Delta\phi_w/\Delta\phi + z_o\Delta\phi_o/\Delta\phi)$$
$$\approx 1 - \alpha$$

or

$$\alpha + \beta \approx 1 \quad (17)$$

where $|1 - z_w|$ and $|1 - z_o|$ are the respective charges of the redox species in the aqueous and organic phases for the reverse ET reaction, considering the above definition of the sign. Thus, the negative dependence of the ET rate constant on the Gibbs energy (i.e., driving force) reported by Nakatani et al.[20c] means a transfer coefficient of the reverse reaction of larger than 1, as reported in the present work, and it can be explained without the introducing of the Marcus inverted region.

Furthermore, we have examined the relationship between $\Delta\phi_w/\Delta\phi$ calculated by this way and the ratio of ionic strength in aqueous phase to that in the organic phase using the published results by several authors. Table 4 provides two series of data for comparison: one using sodium chloride (NaCl) as the aqueous supporting electrolyte and tetrahexyammonium perchlorate ($THAClO_4$) as the organic supporting electrolyte, the other using lithium sulfate (Li_2SO_4) and $THAClO_4$, respectively, and the organic solvents are both DCE. In both of the two series of data, the calculated $\Delta\phi_w/\Delta\phi$ decrease with the ratio of ionic strength in aqueous phase to that in organic phase, which is in accordance with the electrostatic theory.[31] The other issue we have examined is the effect of the dielectric constant of the organic solvent. As shown in Table 5, nitrobenzene, with a larger dielectric constant than DCE, gives a larger value of $\Delta\phi_w/\Delta\phi$. The applications of eq 16 can provide results qualitatively agreeing with the prediction of the simple electrostatic theory, and they support that the Frumkin effect can play an important role in the potential dependence of the ET rate constant at a L/L interface and that the assumption that the potential drop in the inner layer can be neglected is acceptable, to some extent.

The difference in α and, consequently, in the calculated values of $\Delta\phi_w/\Delta\phi$ between Fc and DiMFc cases is another interesting question. We think it may be a consequence of the different potential range at which the interface is biased. In fact, $\Delta\phi_w/\Delta\phi$ varies with the Galvani potential difference according to a simulation based on the Gouy−Chapman theory.[31] It is only in a narrow potential range that α and $\Delta\phi_w/\Delta\phi$ should be expected to keep at a constant value. However, it is still not clear that the difference in α is caused entirely by this effect, and quantitative calculations based on the potential of zero charge and electrostatic theory need to be carried out to clarify this issue.

Conclusions

We have investigated the potential dependence of the ET reactions between $DiMFc^+/Fc^+$ and $Fe(CN)_6^{4-}$ at the polarized W/NPOE interface using the SECM feedback mode. The transfers of $DiMFc^+/Fc^+$ at the W/NPOE interface and their possible effect on the ET process were also studied by micropipet voltammetry. By selecting suitable DF ranges, the effect of IT on the ET processes can be avoided in the SECM kinetic rate constant measurements. The abnormally large values of the transfer coefficients experimentally obtained were discussed and attributed to the Frumkin effect on both sides of the interface. Other abnormal results reported by several authors could also be explained solely by this simplified model based on the Frumkin effect and Girault−Schiffrin interfacial model. The potential distributing at a liquid/liquid interface could be conveniently deduced from the apparent transfer coefficients, assuming that the potential drop in the inner layer could be neglected and the results were in qualitative agreement with the electrostatic theory. The next work is to implement systemic and quantitative research on the potential distribution in the three layers, including the inner one based on the potential of zero charge and electrostatic theory. Moreover, the difference in α values between Fc and DiMFc systems is yet to be elucidated.

Acknowledgment. Financial support for this work from the National Natural Science Foundation of China (20735001, 20628506), the Foundation of Doctoral Programs of the Ministry

of Education of China, and the special 985 Project of Peking University is gratefully acknowledged.

References and Notes

(1) (a) For reviews of electron-transfer reactions at ITIES, see: Girault, H. H. In *Modern Aspects of Electrochemistry*; Bockris, J. O'M., Conway, B. E., White, R. E., Eds.; Plenum Press: New York, 1993; Vol. *25*, p 1. (b) Samec, Z.; Kakiuchi, T. In *Advances in Electrochemical Science and Electrochemical Engineering*; Gerischer, H., Tobias, C. W., Eds.; VCH: New York, 1995; Vol. 4, p 297. (c) Liu, B.; Mirkin, M. V. *Anal. Chem.* **2001**, *73*, 670A. (d) Fermin, D. J.; Lahtinen, R. In *Liquid Interfaces in Chemical, Biological, and Pharmaceutical Applications*; Volkov, A. G., Ed.; Marcel Dekker: New York, 2001; p 179.

(2) (a) Hanzlik, J.; Samec, Z.; Hovorka, J. *J. Electroanal. Chem.* **1987**, *216*, 303. (b) Samec, Z.; Marecek, V.; Weber, J. *J. Electroanal. Chem.* **1979**, *96*, 245. (c) Geblewicz, G.; Schiffrin, D. J. *J. Electroanal. Chem.* **1988**, *244*, 27. (d) Cai, C.; Mirkin, M. V. *J. Am. Chem. Soc.* **2006**, *128*, 171.

(3) Cheng, Y.; Schiffrin, D. J. *J. Chem. Soc., Faraday Trans.* **1993**, *89*, 199.

(4) (a) Shi, C.; Anson, F. C. *J. Phys. Chem. B* **1998**, *102*, 9850. (b) Barker, A. L.; Unwin, P. R. *J. Phys. Chem. B* **2000**, *104*, 2330. (c) Shi, C.; Anson, F. C. *J. Phys. Chem. B* **2001**, *105*, 8963. (d) Lu, X.; Nan, M.; Zhang, H.; Liu, X.; Yuan, H.; Yang, J. *J. Phys. Chem. C* **2007**, *111*, 14998.

(5) For review of MEMED studies of ET at the ITIES, see Guo, S-X.; Unwin, P. R.; Whitworth, A. L.; Zhang, J. *Prog. React. Kinet. Mech.* **2004**, *29*, 43.

(6) (a) Ding, Z.; Fermín, D. J.; Brevet, P. F.; Girault, H. H. *J. Electroanal. Chem.* **1998**, *458*, 139. (b) Eugster, N.; Fermín, D. J.; Girault, H. H. *J. Phys. Chem. C* **2002**, *106*, 3428.

(7) (a) For reviews of SECM studies of ET at the ITIES, see Barker, A. L.; Gonsalves, M.; Unwin, P. R. *Anal. Chim. Acta* **1999**, *385*, 223. (b) Mirkin, M. V.; Tsionsky, M. In *Scanning Electrochemical Microscopy*; Bard, A. J., Mirkin, M. V., Eds.; Marcel Dekker: New York, 2001; p 299. (c) Amemiya, S.; Ding, Z.; Zhou, J.; Bard, A. J. *J. Electroanal. Chem.* **2000**, *483*, 7. (d) Lu, X.; Wang, Q.; Liu, X. *Anal. Chim. Acta* **2007**, *601*, 10.

(8) (a) Solomon, T.; Bard, A. J. *J. Phys. Chem.* **1995**, *99*, 17487. (b) Wei, C.; Bard, A. J.; Mirkin, M. V. *J. Phys. Chem.* **1995**, *99*, 16033. (c) Tsionsky, M.; Bard, A. J.; Mirkin, M. V. *J. Phys. Chem.* **1996**, *100*, 17881. (d) Tsionsky, M.; Bard, A. J.; Mirkin, M. V. *J. Am. Chem. Soc.* **1997**, *119*, 10785. (e) Ding, Z.; Quinn, B. M.; Bard, A. J. *J. Phys. Chem. B* **2001**, *105*, 6367.

(9) (a) Marcus, R. A. *J. Phys. Chem.* **1990**, *94*, 4152. (b) Marcus, R. A. *J. Phys. Chem.* **1991**, *95*, 2010.

(10) (a) Liu, B.; Mirkin, M. V. *J. Am. Chem. Soc.* **1999**, *121*, 8352. (b) Liu., B.; Mirkin, M. V. *J. Phys. Chem. B* **2002**, *106*, 3933.

(11) (a) Zhang, J.; Barker, A. L.; Unwin, P. R. *J. Electroanal. Chem.* **2000**, *483*, 95. (b) Zhang, J.; Unwin, P. R. *J. Phys. Chem. B* **2000**, *104*, 2341. (c) Zhang, J.; Unwin, P. R. *J. Chem. Soc., Perkin Trans. 2* **2001**, 1608. (d) Zhang, J.; Unwin, P. R. *Phys. Chem. Chem. Phys.* **2002**, *4*, 3820. (e) Li, F.; Whitworth, A. L.; Unwin, P. R. *J. Electroanal. Chem.* **2007**, *602*, 70.

(12) (a) Barker, A. L.; Macpherson, J. V.; Slevin, C. J.; Unwin, P. R. *J. Phys. Chem. B* **1998**, *102*, 1586. (b) Barker, A. L.; Unwin, P. R.; Amemiya, S.; Zhou, J.; Bard, A. J. *J. Phys. Chem.B* **1999**, *103*, 7260. (c) Barker, A. L.; Unwin, P. R.; Zhang, J. *Electrochem. Commun.* **2001**, *3*, 372.

(13) (a) Zhang, Z.; Yuan, Y.; Sun, P.; Su, B.; Guo, J.; Shao, Y.; Girault, H. H. *J. Phys. Chem. B* **2002**, *106*, 6713. (b) Sun, P.; Li, F.; Chen, Y.; Zhang, M.; Zhang, Z.; Gao, Z.; Shao, Y. *J. Am. Chem. Soc.* **2003**, *125*, 9600.

(14) Liljeroth, P.; Quinn, B. M.; Kontturi, K. *Langmuir* **2003**, *19*, 5121.

(15) (a) Katano, H.; Maeda, K.; Senda, M. *J. Electroanal. Chem.* **1995**, *396*, 391. (b) Schmickler, W. *J. Electroanal. Chem.* **1997**, *428*, 123.

(16) Girault, H. H.; Schiffrin, D. J. *J. Electroanal. Chem.* **1988**, *244*, 15.

(17) Liu, B.; Mirkin, M. V. *J. Phys. Chem. B* **2002**, *106*, 3933.

(18) Shao, Y.; Mirkin, M. V.; Rusling, J. F. *J. Phys. Chem. B* **1997**, *101*, 3202.

(19) (a) Laforge, F. O.; Kakiuchi, T.; Shigematsu, F.; Mirkin, M. V. *J. Am. Chem. Soc.* **2004**, *126*, 15380. (b) Laforge, F. O.; Kakiuchi, T.; Shigematsu, F.; Mirkin, M. V. *Langmuir* **2006**, *22*, 10705.

(20) (a) Quinn, B.; Lahtinen, R.; Murtomäki, L.; Kontturi, K. *Electrochim. Acta* **1998**, *44*, 47. (b) Laaksonen, T.; Ahonen, P.; Kontturi, K.; Murtomäki, L. *J. Electroanal. Chem.* **2005**, *575*, 75. (c) Nakatani, K.; Yamashita, J.; Negishi, T.; Osakai, T. *J. Electroanal. Chem.* **2005**, *575*, 27.

(21) Studies on ion transfer at the W/NPOE interface are much more extensive than those on electron transfer. Here are some examples: (a) Semac, Z.; Langmaier, J.; Trojánek, A. *J. Electroanal. Chem.* **1997**, *426*, 37. (b) Quinn, B.; Lahtinen, R.; Kontturi, K. *J. Electroanal. Chem.* **1997**, *436*, 285. (c) Wilke, S.; Zerihun, T. *J. Electroanal. Chem.* **2001**, *515*, 52. (d) Gulaboski, R.; Galland, A.; Bouchard, G.; Caban, K.; Kretschmer, A.; Carrupt, P. A.; Stojek, Z.; Girault, H. H.; Scholz, F. *J. Phys. Chem. B* **2004**, *108*, 4565.

(22) (a) Li, F.; Chen, Y.; Zhang, M.; Jing, P.; Gao, Z.; Shao, Y. *J. Electroanal. Chem.* **2005**, *579*, 89. (b) Shao, Y.; Weber, S. W. *J. Phys. Chem.* **1996**, *100*, 14714.

(23) (a) Bard, A. J.; Fan, F.-R. F.; Mirkin, M. V. In *Electroanalytical Chemistry*; Bard, A. J., Ed.; Marcel Dekker: New York, 1994; Vol. 18. (b) Bard, A. J.; Fan, F.-R. F.; Mirkin, M. V. In *Physical Electrochemistry: Principles, Methods and Applications*; Rubinstein, I., Ed.; Marcel Dekker: New York, 1995. (c) Wightman, R. M.; Wipf, D. O. In *Electroanalytical Chemistry*; Bard, A. J., Ed.; Marcel Dekker: New York, 1989.

(24) Martin, R. D.; Unwin, P. R. *Anal. Chem.* **1998**, *70*, 276.

(25) (a) Hanzlík, J.; Samec, Z.; Hovorka, J. *J. Electroanal. Chem.* **1987**, *216*, 303. (b) Zhang, J.; Slevin, C. J.; Unwin, P. R. *Chem. Commun.* **1999**, 1501. (c) Barker, A. L.; Unwin, P. R. *J. Phys. Chem. B.* **2001**, *105*, 12019.

(26) Chen, Y.; Gao, Z.; Li, F.; Ge, L.; Zhang, M.; Zhan, D.; Shao, Y. *Anal. Chem.* **2003**, *74*, 6593.

(27) Cunnane, V. J.; Geblewicz, G.; Schifferin, D. J. *Electrochim. Acta* **1995**, *40*, 3005.

(28) Amphlett, J. L.; Denuault, G. *J. Phys.Chem. B* **1998**, *102*, 9946.

(29) (a) Martin, R. D.; Unwin, P. R. *J. Electroanal. Chem.* **1997**, *439*, 123. (b) Buzzeo, M. C.; Klymenko, O. V.; Wadhawan, J. D.; Hardacre, C.; Seddon, K. R.; Compton, R. G. *J. Phys. Chem. A* **2003**, *107*, 8872. (c) Evans, R. G.; Klymenko, O. V.; Saddoughi, S. A.; Hardacre, C.; Compton, R. G. *J. Phys. Chem. B* **2004**, *108*, 7878. (d) Evans, R. G.; Compton, R. G. *Chem. Phys. Chem.* **2006**, *7*, 488. (e) Ghilane, J.; Lagrost, C.; Hapiot, P. *Anal. Chem.* **2007**, *79*, 7383.

(30) (a) Bard, A. J.; Faulkner, L. R. *Electrochemical Methods*, 2nd ed.; Wiley: New York, 2001; p. 103. (b) Bard, A. J.; Faulkner, L. R. *Electrochemical Methods*, 2nd ed.; Wiley: New York, 2001; p 121. (c) Bard, A. J.; Faulkner, L. R. *Electrochemical Methods*, 2nd ed.; Wiley: New York, 2001; p 571.

(31) Girault, H. H.; Schiffrin, D. J. *J. Electroanal. Chem.* **1985**, *195*, 213.

JP802435M